

**WIND TUNNEL EXPERIMENT OF  
AEROELASTIC FLUTTER**

**by**

**MAH CHUEN TAK**

**Thesis submitted in fulfilment of the requirements for the Bachelor Degree of  
Engineering (Honours) (Aerospace Engineering)**

**June 2018**

## ENDORSEMENT

I, Mah Chuen Tak hereby declare that all corrections and comments made by the supervisor and examiner have been taken consideration and rectified accordingly.

---

(Signature of Student)

Date:

---

(Signature of Supervisor)

Name:

Date:

---

(Signature of Examiner)

Name:

Date:

## DECLARATION

This thesis is the result of my own investigation, except where otherwise stated and has not previously been accepted in substance for any degree and is not being concurrently submitted in candidature for any other degree.

---

(Signature of Student)

Date:

## ACKNOWLEDGEMENTS

Firstly, I would like to thank my parents for supporting me in term of financial and mentally to enable me to continue my study until the university. Without their support I would not able to complete my study until this level.

Next, a special thanks to my fellow friends and coursemates who give a helping hand when I needed. Even some idea of solving the problem is much appreciated. Without their helps and ideas, the research cannot be completed by me.

The staff and technician for School of Aerospace Engineering USM are much appreciated. Thanks to their help in fabricating and professional comment on the fabrication. As they provided professional technique and teach me a lot of technique and new knowledge to me which cannot be learnt in class room that greatly help me in the fabrication of model and rigs.

Lastly, I would like to express my sincere appreciation to my supervisor Dr Norizham bin Abdul Razak. He has been guiding me for the research and put in a lot of effort in teaching me. When I faced some problems he will not directly provide me the solution. He will teach me how to analyse the problem and let me to find out the solution by my own. This is a good teaching method to train me to think like an engineer which is something that I have learnt from the research besides the knowledge. He also giving me moral support in the research which keeps me from giving up to continue put all my effort to finish this project that full of obstacles.

# **WIND TUNNEL EXPERIMENT OF AEROELASTIC FLUTTER**

## **ABSTRACT**

In this work, flutter behaviour of NACA 6409 is investigated using wind tunnel. The plunging and pitching oscillation of the wing is being observed to determine the dynamic instability point. The elastic axis will be manipulated in the experiment where the position of the elastic axis was varied at 25% 50% and 75% of the wing chord to determine the critical flutter speed. The effects on flutter speed at different elastic axis was discussed and analysed to explain the phenomenon. The method of designing and fabrication of the wing model and rig was presented step by step in the thesis. In the experiment the results show that the flutter speed for the elastic axis at 25% of the wing chord is the highest which is 17.84 m/s and follow by the elastic axis at 50% of the wing chord with the flutter speed of 16.36 m/s and lastly is the elastic axis at 75% of the wing chord with the flutter speed of 13.34 m/s. The causes affecting the flutter speed is also discussed. Then flutter suppression experiment was conducted. Active control method using aileron was employed in this research to evaluate the possibility in suppressing flutter oscillation. Autopilot system was installed on the rig of the experiment. The autopilot consisted of a gyro sensor in which it detects the pitching motion of the wing. The idea of the suppression method is to use the autopilot system to detect the pitching motion, and generate signal to be sent to the servo for controlling the motion. The signal is the response that is generated by the PID controller system in the autopilot. The flutter suppression experiment was carried out at the flutter speed of the elastic axis at 50% of the wing chord. The results showed that flutter was suppressed by the autopilot system.

# **EKSPERIMEN KIBARAN DENGAN MENGGUNAKAN TEROWONG ANGIN**

## **ABSTRAK**

Dalam karya ini, tingkah laku NACA 6409 diselidiki menggunakan terowong angin. Gerakan getaran terjun dan angguk diperhatikan untuk menentukan mod getaran sayap. Paksi anjal akan dimanipulasi dalam eksperimen di mana kedudukan paksi anjal akan berubah pada 25% 50% dan 75% dari kord sayap untuk menentukan kelajuan kritikal kibar. Kesan pada kelajuan kibar pada paksi elastik yang berbeza akan dibincangkan dan dianalisis untuk menentukan sebab-sebab hasil yang diperolehi. Kaedah rekabentuk dan pembuatan model sayap dan rig akan dibentangkan secara berperingkat dalam tesis. Hasil ujikaji menunjukkan bahawa kelajuan kibar untuk paksi anjal pada 25% dari kord sayap adalah tertinggi iaitu 17.84 m / s dan diikuti oleh paksi anjal pada 50% dari kord sayap dengan kelajuan berkecepatan 16.36 m / s dan terakhir ialah paksi elastik pada 75% daripada kord sayap dengan kelajuan berkecepatan 13.34 m / s. Punca-punca yang menjejaskan kelajuan berkecepatan tinggi dibincangkan dengan jelas di bab 4. Selepas itu, ujikaji Penindasan kibar dilakukan. Kaedah kawalan aktif menggunakan aileron dinilai dalam penyelidikan untuk menyiasat kebolehan penindasan kibar. Sistem kawalan Autopilot dipasang pada pelantar percubaan. Autopilot terdiri daripada meter giro di dalamnya yang dapat mengesan momen angguk sayap. Idea kaedah penindasan adalah dengan menggunakan autopilot untuk mengesan and menindas mod angguk dan autopilot itu sendiri akan menghasilkan isyarat dan dihantar ke servo. Isyarat adalah tindak balas yang dihasilkan oleh pengawal PID dalam autopilot. Eksperimen penindasan bergetar dilakukan pada kelajuan putaran paksi elastik pada 50% kord sayap. Hasil penyelidikan untuk penindasan flutter berjaya dilakukan oleh sistem autopilot.

## TABLE OF CONTENTS

<b>ENDORSEMENT</b>	<b>I</b>
<b>DECLARATION</b>	<b>II</b>
<b>ACKNOWLEDGEMENTS</b>	<b>III</b>
<b>ABSTRACT</b>	<b>IV</b>
<b>ABSTRAK</b>	<b>V</b>
<b>LIST OF FIGURES</b>	<b>VII</b>
<b>LIST OF TABLES</b>	<b>X</b>
<b>LIST OF ABBREVIATIONS</b>	<b>XI</b>
<b>LIST OF SYMBOLS</b>	<b>XII</b>
<b>CHAPTER 1 INTRODUCTION</b>	<b>1</b>
1.1 Motivation of the research	8
1.2 Research Objective	9
1.3 Thesis Organization	9
<b>CHAPTER 2 LITERATURE REVIEW</b>	<b>11</b>
2.1 Aeroelastic behaviour accident	11
2.2 Research on flutter analysis	13
2.3 2-dimension nonlinear flutter model theory	19
<b>CHAPTER 3 METHODOLOGY</b>	<b>24</b>
3.1 Design and Fabrication of Wing section	25
3.2 Design and Fabrication of flutter Rigs	34
3.3 Wind Tunnel Testing	41
<b>CHAPTER 4 RESULT AND DISCUSSION</b>	<b>46</b>
4.1 Elastic axis Experiment	46
4.2 Flutter suppression experiment	58
<b>CHAPTER 5 CONCLUSION AND RECOMMENDATIONS</b>	<b>60</b>
5.1 Conclusion	60
5.2 Recommendations	60
<b>REFERENCES</b>	<b>62</b>
<b>APPENDICES</b>	<b>64</b>
APPENDIX A. NACA 6409 AIRFOIL COORDINATE	64
APPENDIX B. PARTS DESIGN FOR CNC HOW WIRE CUTTER	66
APPENDIX C. MATLAB Coding for Plotting Amplitude Graph	69
APPENDIX D. MATLAB Coding for Plotting Frequency-Velocity Graph	70

## LIST OF FIGURES

Figure 1.1:Aeroelasticity Relation	1
Figure 1.2 : Pressure Distribution On Airfoil Due To Divergence	2
Figure 1.3: Pressure Distribution On Airfoil Due To Shock Buffet	3
Figure 1.4: Pressure Distribution On Airfoil Due To Aileron Buzz	4
Figure 1.5: Flow Diagram Of Wake Vortex Flutter	6
Figure 2.1: Schematic Of The Two Degree Of Freedom Airfoil Model	19
Figure 3.1: Methodology Flow Chart	25
Figure 3.2: Wind Tunnel Dimension	26
Figure 3.3: Perspex Ribs	27
Figure 3.4: Cnc Hot Wire Cutter Design	28
Figure 3.5: Assumble Cnc Hot Wire Cutter	29
Figure 3.6: (A) Assemble Of Stepper Motor With Stepper Motor Drive And (B) Schematic Connection	30
Figure 3.7: Trimmed Cupboard For Reference	31
Figure 3.8: Wing And Aileron	32
Figure 3.9: Installation Of Servo And Control Horn	33
Figure 3.10: Final Assembly Of Wing	33
Figure 3.11: Initial Rig Design	34
Figure 3.12: New Rig Design	35
Figure 3.13: Hollow Alluminium Rig	36
Figure 3.14: Special Design Bracket	37
Figure 3.15: Rig Setup	37



Figure 3.16: 3d Printed Wing Holder	38
Figure 3.17: 3d Printed Wing Holder Spoiled	39
Figure 3.18: Steel Wing Holder	39
Figure 3.19: Slotted Test Section Window	40
Figure 3.20: Test Setup For Wind Tunnel Flutter Experiment	41
Figure 3.21: Sn-Imu5d-Lc Sensor	42
Figure 3.22: Ni Daq Usb 6001	42
Figure 3.23: Labview Block Diagram	43
Figure 3.24: Display Window	43
Figure 3.25: Position Of The Motion Sensor	44
Figure 3.26: Position Of Installed Autopilot System	45
Figure 4.1: Vibration Response Graph Of Elastic Axis At Position 25% For Airspeed 7.34 M/S	48
Figure 4.2: Vibration Response Graph Of Elastic Axis At Position 25% For Airspeed 15.54 M/S	49
Figure 4.3: Vibration Response Graph For Elastic Axis At Position 25% At Flutter Speed 17.84 M/S	50
Figure 4.4: Frequency Vs Velocity Graph Of Elastic Axis At Position 25%	50
Figure 4.5: Damping Ratio Vs Velocity Graph Of Elastic Axis At Position 25%	51
Figure 4.6: Frequency Vs Velocity Graph Of Elastic Axis At Position 50%	52
Figure 4.7: Frequency Vs Velocity Graph Of Elastic Axis At Position 75%	53
Figure 4.8: Vibration Response Graph Of Elastic Axis At Position 50% For Airspeed 7.34 M/S	54
Figure 4.9: Vibration Response Graph Of Elastic Axis At Position 50% For Airspeed 15.54 M/S	55

Figure 4.10: Vibration Response Graph Of Elastic Axis At Position 50% For Airspeed 16.36 M/S	55
Figure 4.11: Damping Ratio Vs Velocity Graph Of Elastic Axis At Position 50%	57
Figure 4.12: Damping Ratio Vs Velocity Graph Of Elastic Axis At Position 75%	57
Figure 4.13: Suppression Response Of The Wing At Flutter Speed	59
Figure 7.1: Y Axis Support Drawing	66
Figure 7.2: Y Axis Motor Holder Drawing	67
Figure 7.3: Y Axis Motor Holder Cap Drawing	68

## LIST OF TABLES

Table 4-1: Parameter For Elastic Axis At 50% Of The Wing	46
Table 4-2: Parameter For Elastic Axis At 25% Of The Wing	46
Table 4-3: Parameter For Elastic Axis At 75% Of The Wing	46
Table 7.1 Naca6409 Coordinate	64

## **LIST OF ABBREVIATIONS**

PID : Proportional, Integration, Differentiation

## LIST OF SYMBOLS

$K_h$	: Bending stiffness
$K_\theta$	: Torsional stiffness
$e_{ac}$	: Distance between aerodynamic centre and elastic axis
$\alpha$	: Angle of attack
$\dot{\alpha}$	: Angle of attack rate
$q$	: Pitch rate
$\bar{q}$	: Dynamic pressure,
$\bar{c}$	: Chord length
$h$	: Plunge velocity
$\theta$	: Pitch velocity
$M_s$	: Mass matrix
$K_s$	: Stiffness matrix
$m$	: Mass
$e$	: Distance between centre of mass and elastic axis
$J$	: System Jacobi matrix
$L_\alpha$	: Aerodynamic lift

$M_a$  : Aerodynamic moment

$C_{L\alpha}$  : Aerodynamic lift coefficient

$C_{M\alpha}$  : Aerodynamic moment coefficient

$S$  : Wing surface area

$V$  : Free stream velocity

$E_L$  : Linear mass normalized stiffness matrix

$E_{NL}$  : Non-linear mass normalized stiffness matrix

$D$  : Mass-normalized damping matrix

$\emptyset$  : Non-linear function

# CHAPTER 1

## INTRODUCTION

Aeroelasticity is the interaction between structural dynamics and unsteady aerodynamic flow over the structure. It is an important area of study for two main reasons. First the interaction can lead to static instability which deals with the static or response typically is the vibration response. Both of the instabilities can result in failure of the structure. Secondly the loads calculated using aeroelastic simulations are significantly different for flexible structures compared to decoupled structural and aerodynamic simulations. This has a significant influence on the design and weight of the structure, and its aerodynamic performance. Therefore it is important to take aeroelasticity effects into account in the design of structures.

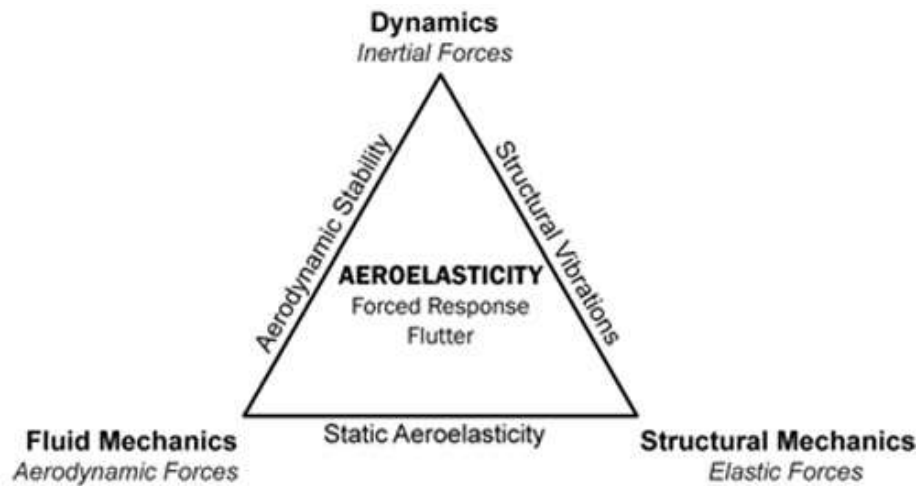


Figure 1.1: Aeroelasticity relation

For static instability, 2 significant aeroelasticity phenomena that will happen are Divergence and Control Reversal. The wing of the aircraft suddenly elastic twisted

until the wing's structure failed is the Divergence phenomena. It occurs due to the lift force produce by the wing causes the wing itself to be twisted on the flexural axis. Hence, it increase the angle of attack of the wing causes the wing to produce a greater lift force and twisted the wing more. This process repeated until it exceeds the restoring force of the structure and the wing break.

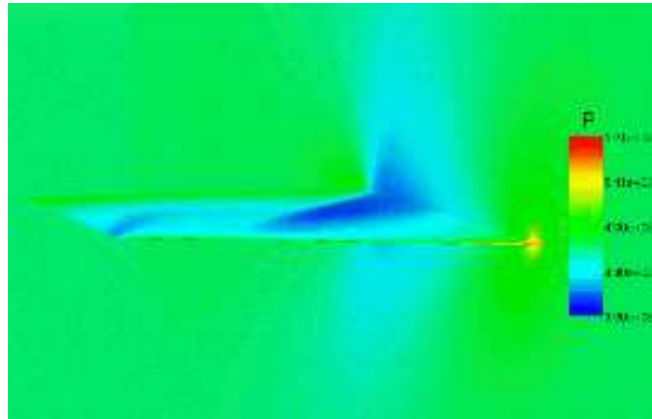


Figure 1.2 : Pressure distribution on airfoil due to divergence

Control surface reversal is the loss or reversal of the expected response of a control surface, due to deformation of the main lifting surface. This phenomena occurs because of aileron deflects downward causes the nose down twisting of the wing which reduces the aileron incidence. The wing twist tends to reduce the increase in lift produced by the aileron deflection.

For dynamic instability, the phenomena that will occur due to it are shock buffet, buffet, aileron buzz and flutter. At transonic flow conditions, beyond critical angles of attack and Mach number, the flow around airfoil exhibits shock-induced flow separation. These flow oscillations can occasionally turn into self-excited limit cycle oscillations of large amplitude or known as transonic buffet or shock buffet.



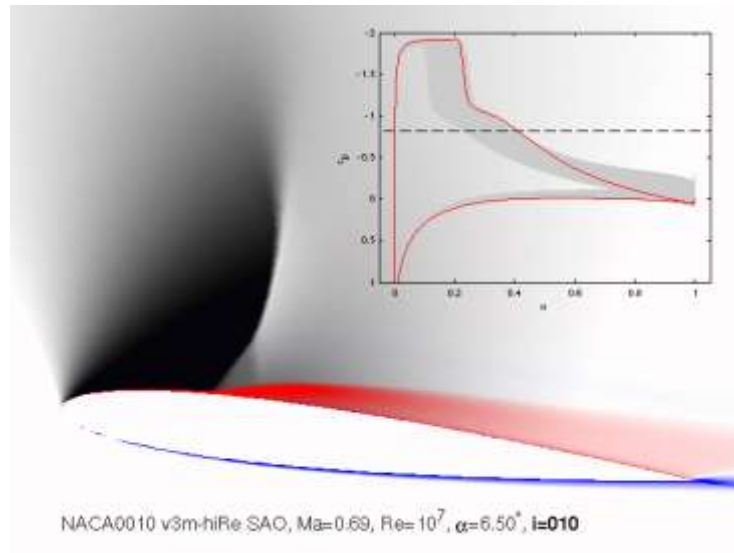


Figure 1.3: Pressure distribution on airfoil due to shock buffet

Buffet is a randomly varying structural response often triggered by intense and chaotic aerodynamic forcing functions associated with stalled or separated flow conditions. Fluctuating pressures present during buffet conditions can cause highly undesirable responses from wings, fuselages, pod-mounted engine nacelles, and empennages. It is caused by a sudden impulse of load increasing which is the aerodynamic force due to turbulence and causes a random forced vibration. Dynamic loads experienced during buffet can lead to pilot fatigue or structural fatigue, resulting in serious reductions in the anticipated structural life of airframe components. Generally it affects the tail unit of the aircraft structure due to air flow downstream of the wing.

Aileron buzz only occurred when the aircraft fly at transonic speed and it is associated with a shockwave on the wing at the position of forward parts of the aileron. When the aileron deflects downward, the flow pass through the upper surface of the wing will be accelerated and the shock becomes more intense and causing a reduction

of pressure in the boundary layer behind the shockwave. Therefore, the aileron tends to suck back to its neutral position due to the difference in pressure. When the aileron deflects upward, the shock intensity decreases, causing the pressure in the boundary layer to increase and tend to push the aileron down to the neutral position. These both sucking and pushing actions on the aileron repeat and cause the occurrence of aileron buzz.

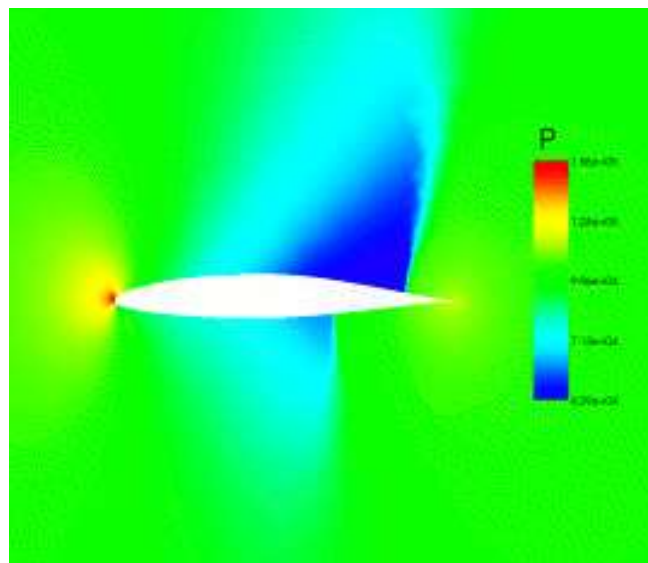


Figure 1.4: Pressure distribution on airfoil due to aileron buzz

Flutter phenomena is a dangerous phenomenon that is encountered in flexible structures which are subjected to aerodynamic forces. Flutter occurs due to the interactions between aerodynamics, stiffness and inertial forces on a structure. It is a self-feeding and potentially destructive vibration where aerodynamic forces on an object couple with the structure's natural frequency and produce rapid periodic motion.

Flutter can occur in any object within a strong flow of fluid, at the condition of there is a positive feedback occurs between the structure's natural vibration and the

aerodynamic forces. The vibration movement of the of the object increases an aerodynamic load which is in turn drives the object to move further.

In an aircraft, as the speed of wind increases, it will increase the aerodynamic excitation to the wing. When the aerodynamic excitation is larger than the natural damping of the wing structural to damp out the motion, it will cause the vibration to increase and resulting in self-exciting oscillation of the wing. The vibration thus build up and re only limited when the aerodynamic or mechanical damping of the object match the energy input, this often results in large amplitudes and can lead to rapid failure of the structure. Therefore flutter characteristic is an important part in aircraft design.

There are few types of flutter behaviour that must be considered in aircraft design. For example, panel flutter, galloping flutter, stall flutter, and classical flutter. Panel flutter occurs when a surface is not adequately supported. The panel is deflected from its original position and causes the formation of vorticity on the surface. Galloping flutter can also be called wake vortex flutter or vortex induced vibration. This phenomena is the motions induced on structure interacting with an external fluid and producing a periodic vortices. The formation of wake vortices at the downstream of the object causes the galloping motion to occur.

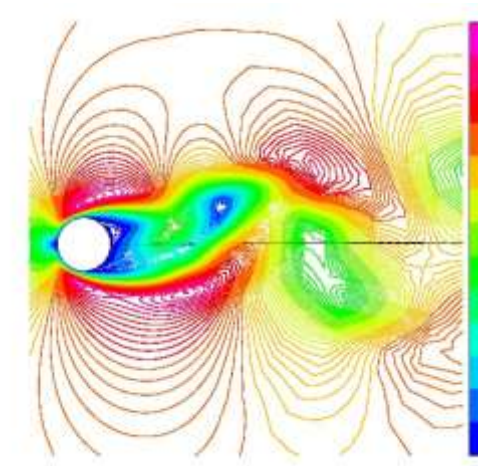


Figure 1.5: Flow diagram of wake vortex flutter

Stall flutter is a torsional mode of flutter that occurs on wings at high loading conditions near the stall speed. It is a type of dynamic instability that takes place when the separation of flow around an airfoil occurs during the whole or part of each cycle of a motion. This phenomenon is a single degree of freedom that is different from the classical flutter.

Classical Flutter is also called as Bending Torsion Flutter. It involves the interactions of a structure's elastic and inertia characteristics with the aerodynamic forces produced by the airflow over the vehicle. It is a self-excited oscillation of the aircraft structure involving energy absorbed from the airstream. When an aircraft's elastic structure is disturbed at speeds below flutter speed, the resulting oscillatory motions decay. When the structure is disturbed at speeds above flutter speed, the oscillatory motions will abruptly increase in amplitude and can rapidly lead to catastrophic structural failure. This phenomenon requires 2 DOF system to manifest.

As flutter phenomena is so dangerous and chaotic, the method to suppress flutter is very important to solve this problem. There are 2 categories for suppressing

flutter which are the passive and active methods. Structural stiffening, mass balancing, dynamic vibration absorber and flight envelope modification are the traditional passive suppressing methods that have been used. While smart material and using control surface are modern active suppressing methods.

Structural stiffening is adding additional structure to stiffen the primary structure which already sufficiently strong to carry normal flight loads. This method will require to redesign the structural of the wing and adding cost and weight to the aircraft as more parts needed to add in to the design to increase the stiffness of the wing.

Mass balancing is being done by rearranging the components within the structure of the wing such as fuel tank, servo actuator and other else. Besides that, it also can be done by adding counter weight to change the centre of mass of the structure. All these are to bring the centre of mass as close as possible to the elastic axis of the wing. As the flutter speed will increase if the centre of mass is close to the elastic axis. However, this method needed to redesign the wing and reduce the aircraft payload capability as weight is added to the aircraft. Moreover, increase in weight will adversely affect manufacturing and acquisition costs, mission performance, and add to operational costs throughout the life of the airplane.

Dynamic vibration absorber can be used to absorb the vibration due to buffer. However, a small and lightweight dynamic vibration absorber is needed in order to be incorporated in the aerodynamic surfaces. Moreover, dynamic vibration absorber is only tailored to specific frequency. Therefore it only can be used to damp a certain frequency of vibration. Hence the use of dynamic vibration absorber has its limitation use for the specific design.

The last passive suppress method is modification of flight envelope. This method is to shrink the flight envelope by lowering the maximum airspeed and altitude of the aircraft and limit the flight regime. This method is a last resort as it will upset the customer and affect the future order from customer.

For active suppressing method, smart material is being used. Smart material such as Piezoelectric material is being used to increase the damping to the structure and reduce the amplitude of the vibration during flutter. By using this method, the flutter speed of the aircraft can be increased by 5% until 10% of the original flutter speed. Using aircraft control surfaces also is one of the active suppress method. The aircraft control surfaces are linked to a computer and sensors in a manner to automatically and immediately limit any unwanted motions or aerodynamic loads on the aircraft structure.

## **1.1 Motivation of the research**

All flexible structures subjected to aerodynamic flow will undergo aeroelastic flutter oscillation and the oscillation can lead to structural failure. Therefore, the parameters that affect the flutter speed are of interest. The question of “how does changing the position of elastic axis of the wing affect the flutter speed” is an important question that needs answer. If flutter does occur, how can aileron been used to suppressed the flutter oscillation using active control approach?

## **1.2 Research Objective**

Since flutter can be catastrophic for aircraft structures, it is important to know the parameters that affect the flutter speed and how can it be suppressed. In this work, the objectives are to:

- i) Evaluate the effect of elastic axis position on the critical flutter speed of NACA 6409 via wind tunnel experiment.
- ii) Evaluate the use of aileron for flutter suppression via active control approach employing Autopilot system.

## **1.3 Thesis Organization**

There are total 5 chapters in this thesis which are break into Introduction, Literature Review, Methodology, Results and Discussion and Conclusion and Recommendation. For the first chapter introduction, a brief definition and understanding of the aeroelasticity behaviour will be introduced and clearly state the objective of the research.

For chapter 2 literature review, some accident cases that previously occurred due to flutter will be studied to have a better understand on the real case scenario which can get idea from it in the be applied in the experiment. Besides that, various method and research that others researchers have been done have also been studied to learn their technique used in conducting the aeroelasticity flutter analysis. The theory of flutter is discussed to provide a theoretical insight of each method on how it used in modelling and analysis.

Chapter 3 is methodology which is provided the steps from designing until the setup of the experiment and how the experiment was run. The chapter will provide a clearly detail description on the designing and fabrication of wing and rig of the experiment. Besides that, the setup of the experiment and each steps of the experiment to achieve the objective have been clearly explained in this chapter.

The result is discussed in chapter 4. The experimental result for the different position of elastic axis is shown and discussed. Moreover, the suppression result for using active control method is also been discussed. The last chapter is the conclusion and recommendation of the research. The chapter will provide a summary of the results and some future recommendation which can improve the accuracy of the experiment as a reference for others researchers.



## **CHAPTER 2**

### **LITERATURE REVIEW**

This chapter present the detail of the study on the past researches and theory that related to this research. Firstly, a few cases study on the aeroelastic behaviour accidents have been done to determine the causes of the phenomena of aeroelasticity. Besides that, the researches that have been done by others researchers also have been studied. Lastly, theory of aeroelasticity behaviour also been presented in the last part of this chapter.

#### **2.1 Aeroelastic behaviour accident**

A few flutter accidents were been studied to identify the causes of flutter occur during the flight. The first accident that studied was Grob spn flutter accident. This was an accident occur during the demonstration flight of the Grob spn with the purpose of demonstrate the aircraft to a group of visitors on the ground at Mindelheim-Mattsies airfield. The aircraft crashed after the pilot loss control of the aircraft due to the elevator experience flutter and the elevator and parts of the horizontal stabilizer break from the aircraft.

The Flutter Analysis Evaluation AC 23.629-1B in conjunction with Certification Specification CS-23 resulted the flutter speed is 313 knots however the result from calculation in accordance with AC 23.629 stated that the flutter speed was 261 knots. Therefore the flutter occurrence was suspect due to excessive speed during the flight as the aircraft was predicted reach the speed 270 knots. Another cause that being predicted was due to the bond holding the retrofit elevator mass balance had

previously failed. In this case, the critical speed range would have shifted towards lower speeds (Flugunfalluntersuchung, 2006).

Nomad aircraft N24-10 is the second accident case that has been studied. The aircraft was crashed and destroyed at 6 August 1976 to carry out flight 128 at Avalon, Victoria. The flight clearance for N22 aircraft by calculation and flight test speed was cleared up to 218 knots. While during the accident, N24-10 had been permitted to fly at 120 knots with wing tips tank full and 170 knots with wing tip tank empty. Witness claimed that when the aircraft on straight climb the tailplane tabs experience flutter and pieces of skin and a section of T strip from the port tail place separate from the aircraft.

In their analysis, 2 types of flutter models have been made which are low frequency symmetric tailplane model and high frequency antisymmetric model. The two models were separated because of the difficulties experienced in calculating unsteady aerodynamics applicable to both the high frequency and the low frequency cases. To justified the model, the flutter speed of other aircraft configuration were been used in this model and compare with actual flight data. The results turn out to be consistence with the flight test experiment.

The analysis results show that in the accident configuration, flutter of the tailplane and tabs could be expected at the speed between 90 knots and 115knots depending on the parameter value used. This flutter critical situation arises from the inertia and aerodynamic effects of T strips added to the trailing edge of the tailplane tabs. Different dimension of the T strips will affect the aerodynamic effect. As in the analysis 2 inch T strips having a lower flutter speed configuration compare to 1 inch T strips. This is derived mainly from the increased inertial effects of the larger T strips.

The investigation came with the conclusion for the accident that flutter could be occurred in the accident configuration at the speed below 120 knots. Flutter phenomena is the primary cause to the accident (BRANCH, 1976).

## **2.2 Research on flutter analysis**

Flutter is not only occurs on aircraft wing, it can occur at any object which interact with fluid flow. As low speed aircrafts need clean airflow over the tail surfaces to have better pitch control. Therefore a T-Tail configuration is preferred for such flying machines due to its geometric location. The aeroelastic problems for T tail is a great concern because of the structurally heavy vertical stabilizer needs to carry the lift producing horizontal tail, which makes T-Tail a structure of concern in the low speed aircraft. Therefore, some experiments have been carried out to determine the flutter phenomena on a T tail model of a conventional aircraft (Samillannu & Upadhya, 2011) . The results for the experiment shows that the critical modes of the T-Tail have not shown any dynamic instability nature at critical flight velocity 141.33m/sec at the Mach range of 0.2 to 0.4 and the total damping for Structural and Aerodynamic of the critical modes are noticed to be around 2%. This result has ensured that the T-Tail is qualified from flutter at maximum diving velocity.

As flutter is a very catastrophic phenomena, researcher have been carried out a lot of method in analysing the flutter speed of the aircraft. Traditional analysis is fabricated an aircraft model and run the experiment in the wind tunnel to get the results. Conventional methods of examining aeroelastic behaviour have relied on a linear approximation of the governing equations of the flow field and/or the structure. However, aerospace systems inherently contain structural and aerodynamic

nonlinearities. Therefore, nonlinear aeroelastic behaviour experiment has been done by Todd O'Neil (O'Neil, 1996) .

Duke aeroelastic group keep design new model and carry out wind tunnel test to evaluate the new theory and computational method Duke aeroelastic group (Tang & H.Dowel, 2016) . The purpose of their experiment is to verify the correlation between theory and experiment. In the past 20 years, they have evaluated total of 6 new theories which are as follow:

1. A high aspect ratio wing model. Several correlation studies for flutter and limit cycle oscillation (LCO) ,limit cycle hysteresis response , gust response for clamped and flexibly suspended models and Flutter/LCO suppression were performed.
2. Wing like plate models, delta wing-store, flapping flag, yawed plate and folding wing. The wing tunnel tests were used to evaluate the von Karman nonlinear plate theory, and a new nonlinear inextensible beam and plate theory and also some high fidelity computation methods. Based on these models several correlation studies for flutter/LCO and gust response studies were performed.
3. Airfoil section with control surface freeplay. The wing tunnel tests were used to evaluate new approaches for the freeplay nonlinear and gust responses including Duke computational codes using the Peter's finite state airload aerodynamic theory, harmonic balance method, and the time marching integration based on state space equations and the ZAERO code based on the computational fluid dynamic (CFD) theory conducted by ZONA Technology, Inc.

4. All-movable tail with freeplay model at the root to similar horizontal tail in the actuating mechanism freeplay nonlinearity of aircraft. Based on this model a computational code has been developed and evaluated.
5. A free-to-roll fuselage flutter model. From measured wind tunnel data, one evaluates the predicted symmetric and anti-symmetric flutter/LCO theory.
6. An experimental oscillating airfoil model at high angles of attack for measuring aerodynamic response. A frequency “Lock-in” phenomenon is found in buffeting flow and compared to the theoretical results. Also, an experimental airfoil model with a partial-span control surface is conducted to measure the flap response of the partial-span induced by the buffeting flow.

Others from experiment, mathematic modelling is also another method to determine the flutter behaviour. Mathematic modelling is translating problems from an application area into tractable mathematical formulations whose theoretical and numerical analysis provides insight, answers, and guidance useful for the originating application (Shibov, 2006). In the article, it provides a few methods in analysing the problem of flutter using mathematic modelling and how to control the flutter phenomena using calculation.

Robust Flutter analysis is a match point solution which is another method that has been done to analyse flutter phenomena. This method uses flight altitude as the perturbation variable in order to obtain a match point solution. The air density and sound speed of standard atmosphere model are approximated as the polynomial function of altitude, such that the flight altitude becomes the single perturbation variable that describes the aeroelastic system (HaiWei & JingLong, 2008) . In the analysis, it took consideration of the uncertainties of generalized stiffness and damping. The uncertain aeroelastic system is then formulated in into linear fraction transformation representation which is suitable for  $\mu$  analysis framework. This method

is suitable for analysing the problem of constant Mach flight as it can provide valuable reference for flight envelope expansion.

Besides that, some experiment on also composite panel has also been carried out by some researcher to study its layer orientation affect the aeroelasticity phenomena (An, et al., 2017). As composite panel is mostly use as the material for manufacture the wing of aircraft. Therefore, the study on the aeroelasticity phenomena is very important. From the research, the researcher tested the thin composite panel by using numerical method (finite element co-rotational theory ) with 2 different sizes of curvature which are  $H/h = 5$  with orientation of the fibre layer of  $[0^\circ/90^\circ/90^\circ]$  and  $H/h = 10$  with the orientation of the fibre layer of  $[0^\circ/90^\circ/90^\circ]$  and  $[45^\circ/45^\circ/45^\circ]$ . The results show that For the Mach number,  $M=0.96$ , the flutter dynamic pressures of the three panels are always relatively large, and the amplitudes of the oscillations are more than 17.5 times the thickness of the panel. For  $M=1.67$ , the panel of  $H/h = 10$  with  $[45^\circ/45^\circ/45^\circ]$  has the lowest flutter dynamic pressure among the three cases. Moreover, under the same dynamic pressure, both the static aeroelastic deformation and the amplitude of the oscillation are lower than the other two panels.

To reduce uncertainty of the results, probabilistic collocation has been used. This technique an uncertainty quantification technique which can efficiently propagate multivariate stochastic input through a simulation code, in this case an eigenvalue-based fluid-structure stability code. The resulting analysis predicts the consequences of an uncertain structure on incidence of utter in probabilistic terms of information that could be useful in planning flight-tests and assessing the risk of structural failure (Dwight, et al., 2011) . In the results for the research, very large flutter altitude variabilities are seen to result from moderate variability in many structural parameters, and this relationship is captured well by a probabilistic representation of uncertainty.

Flutter suppression has been categorized into 2 which are passive suppression and active suppression. Passive suppression is to modify the structure, thereby either eliminating undesirable excitation of structural characteristics or ensuring that the undesirable phenomena occur only at conditions beyond the flight envelope such as structural strengthening, mass balancing, and dynamic vibration absorber. Structural strengthening is to increase the stiffness of the structural. While mass balancing is to move the centre of gravity as close to the elastic axis. Dynamic vibration absorber is another passive suppress method for flutter. However, it usually been used on infrastructure such as bridge to suppress flutter (M.Gu, et al., 1998). In the result of the research, it clearly showed that tuned mass damper increase the flutter speed significantly. The tuned mass damper with more than 5.6% ratio of mass inertia moment increased the critical flutter speed on the bridge model with wind screen by more than 40% but this effect only proportional until the ration of mass inertia moment is lower than 10%. As more than 10%, the experimental and numerical results show the efficiency of control tend to decrease. However, this method is not suitable for aircraft structure as it added a lot of mass to the aircraft which lower the profit of the airline. Therefore, it not preferable, however on others structure that will encounter with flutter this is a very effective suppression method. However, DVA was also implied in aircraft in F-18 tail to absorb buffet.

For active control, smart material such as piezoelectric is often been used to increase the damping and reduce vibration amplitude (deSousa, et al., 2017). NASA has carried out an experimental and analytical investigation to evaluate the usefulness of piezoelectric in suppressing flutter. The experiment of NASA is to use piezo electric to control plunging and pitching moment to suppress the flutter. Beside experimental, analytic results have also been done to compare with the experimental results.

Experimental results from several system identification tests determined the natural frequency of the plunge mode to be 7.9 Hz and that of the pitch mode to be 11.1 Hz. The structural damping associated with these modes was also determined. The open loop flutter speed was measured at 580 in/sec. The analytical prediction was conservative by 3.5 percent.

Closed loop utter testing was performed and a flutter speed of 697 in/sec was obtained. This represents a 20-percent improvement from the open loop case. The analytical prediction of closed loop flutter speed was conservative by 7.6 percent (Heeg, 1993) .

Besides NASA, University of Sao Paulo also has carried out the similar experiment on using smart material suppressing flutter. They have investigated the combined effects of semi-passive control using shunted piezoelectric material and passive pseudoelastic hysteresis of shape memory springs on the aeroelastic behaviour of a typical section. In their experiment, the individual effects of each nonlinear mechanism on the aeroelastic behaviour of the typical section were first verified and then combined the effects of semi-passive piezoelectric control and passive shape memory alloy springs on the post-critical behaviour of the system were discussed to show how it suppress flutter. The experimental result shows that the range of post-flutter airflow speeds with stable limit cycle oscillations is significantly increased due to the combined effects of both sources of energy dissipation, providing an effective and autonomous way to modify the behaviour of aeroelastic systems using smart materials.



### 2.3 2-dimension nonlinear flutter model theory

2-dimension flutter is the study of the a simple 2 dimension airfoil constraint to two degree of freedom which are the plunge,  $h$  and pitch moment,  $\theta$ . Lagrange's method is being used to develop the structural force as the Figure 2.1.

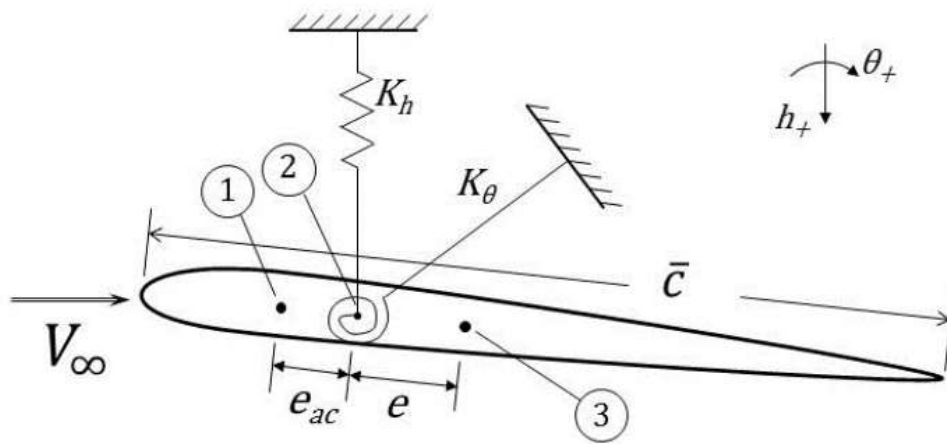


Figure 2.1: Schematic of the Two Degree of Freedom Airfoil Model

Force and moment contributions due to the dislocation of the centre of gravity from the elastic axis are taken account in the calculation. Structural restoring forces are applied at the elastic model to decouple the stiffness in plunge,  $K_h$  and pitch,  $K_\theta$ . With the frame of reference located at the elastic axis, the dislocation of the centre of mass introduces a coupling of pitch and plunge inertia sometimes referred to as static unbalance. The energy based approach determines the system equations of motion, resulting in a standard set of equations where the structural forces are balanced against the existing aerodynamic forces.

$$M_s \begin{bmatrix} \ddot{h} \\ \ddot{\theta} \end{bmatrix} + K_s \begin{bmatrix} h \\ \theta \end{bmatrix} = F_{aero} \quad (2.1)$$

where,

$$M_s = \begin{bmatrix} m & -me \\ -me & me^2 + J \end{bmatrix} \quad K_s = \begin{bmatrix} K_h & 0 \\ 0 & K_\theta \end{bmatrix} \quad F_{aero} = \begin{bmatrix} -L_a \\ M_a \end{bmatrix}$$

The aerodynamic forces and moments act as forcing function to the elastic structure. To capture the unsteady term of the fluid flow response by these forces and moments is through the use of classical non-dimensional force and moment coefficient which valid for both steady and unsteady aerodynamics. Then, the aerodynamic states of angle of attack,  $\alpha$ , angle of attack rate,  $\dot{\alpha}$ , and pitch rate,  $q$  are determined using the obtained force and moment.

$$L_a = \bar{q}S(C_{L\alpha}\alpha + C_{L\dot{\alpha}}\dot{\alpha} + C_{Lq}q) \quad (22)$$

$$M_a = \bar{q}S\bar{c}(C_{M\alpha}\alpha + C_{M\dot{\alpha}}\dot{\alpha} + C_{Mq}q) + \bar{q}Se_{ac}(C_{L\alpha}\alpha + C_{L\dot{\alpha}}\dot{\alpha} + C_{Lq}q) \quad (2.3)$$

where  $\bar{q}$  is dynamic pressure,  $\bar{c}$  is the chord length and  $e_{ac}$  is the distance from aerodynamic centre to the elastic axis. Moment due to the dislocation of aerodynamic centre and elastic axis is included in the calculation. The unsteady aerodynamic response of the airfoil was captured by first order term in  $\alpha$  and  $\theta$ . To provide the full aeroelastic model, the dependent variables of the aerodynamic equations are converted to the state variables of the structure by making the following substitution:

$$\alpha = \theta + \frac{\dot{h}}{V} \quad (2.4)$$

$$\dot{\alpha} = \dot{\theta} + \frac{\ddot{h}}{V} \quad (2.5)$$

$$q = \dot{\theta} \quad (2.6)$$

This allows the coupled aeroelastic model to be resolved to a common set of state variables,

$$L_a = \bar{q}S[C_{L\alpha}(\theta + \frac{\dot{h}}{V}) + C_{L\dot{\alpha}}(\dot{\theta} + \frac{\dot{h}}{V}) + C_{Lq}(\dot{\theta})] \quad (2.7)$$

$$M_a = \bar{q}S\bar{c}[C_{M\alpha}(\theta + \frac{\dot{h}}{V}) + C_{M\dot{\alpha}}(\dot{\theta} + \frac{\dot{h}}{V}) + C_{Mq}(\dot{\theta})] + \bar{q}Se_{ac}[C_{L\alpha}(\theta + \frac{\dot{h}}{V}) + (\dot{\theta} + \frac{\dot{h}}{V}) + C_{Lq}(\dot{\theta})] \quad (2.8)$$

Plunge velocity,  $h$  and pitch velocity,  $\theta$  remain as first order but the aerodynamic force equations represented by structural state variables produce aerodynamic contributions to the apparent mass, stiffness and damping of the coupled system.

$$F_{aero} = M_{app} \begin{bmatrix} \ddot{h} \\ \ddot{\theta} \end{bmatrix} + B_a \begin{bmatrix} \dot{h} \\ \dot{\theta} \end{bmatrix} + K_a \begin{bmatrix} h \\ \theta \end{bmatrix} \quad (2.9)$$

where,

$$M_{app} = \bar{q}S \begin{bmatrix} \frac{-C_{L\dot{\alpha}}}{V} & 0 \\ \frac{\bar{c}C_{M\dot{\alpha}} + e_{ac}C_{L\dot{\alpha}}}{V} & 0 \end{bmatrix}$$

$$K_a = \bar{q}S \begin{bmatrix} 0 & C_{L\alpha} \\ 0 & cC_{M\alpha} + e_{ac}C_{L\alpha} \end{bmatrix}$$

$$B_a = \bar{q}S \begin{bmatrix} \frac{-C_{L\alpha}}{V} & -(C_{L\dot{\alpha}} + C_{Lq}) \\ \frac{\bar{c}C_{M\alpha} + e_{ac}C_{L\alpha}}{V} & \bar{c}(C_{M\dot{\alpha}} + C_{Mq}) + e_{ac}(C_{L\dot{\alpha}} + C_{Lq}) \end{bmatrix}$$

Combine equation 2.1 and 2.5 resulted a couple system of  $h$  and  $\theta$ .

$$(M_s - M_{app}) \begin{bmatrix} \ddot{h} \\ \ddot{\theta} \end{bmatrix} = B_a \begin{bmatrix} \dot{h} \\ \dot{\theta} \end{bmatrix} + (K_a - K_s) \begin{bmatrix} h \\ \theta \end{bmatrix} \quad (2.10)$$

$$\begin{bmatrix} \ddot{h} \\ \ddot{\theta} \end{bmatrix} = (M_s - M_{app})^{-1} B_a \begin{bmatrix} \dot{h} \\ \dot{\theta} \end{bmatrix} + (M_s - M_{app})^{-1} (K_a - K_s) \begin{bmatrix} h \\ \theta \end{bmatrix}$$

$$\begin{bmatrix} \ddot{h} \\ \ddot{\theta} \end{bmatrix} = D \begin{bmatrix} \dot{h} \\ \dot{\theta} \end{bmatrix} + E \begin{bmatrix} h \\ \theta \end{bmatrix}$$

Assign the state vector  $x = [h \ \theta \ \dot{h} \ \dot{\theta}]^T = [x_1 \ x_2 \ x_3 \ x_4]^T$  to obtain state space representation. Therefore,

$$\dot{x} = \begin{bmatrix} 0 & I \\ E & D \end{bmatrix} x \quad (2.11)$$

The nonlinear structural stiffness behaviour is contained in the original  $K_\theta$  term, which in turn is now embedded in the E matrix derived above. Specifically,

$$E_{11} = \frac{-K_h V(m e^2 + J)}{|M_s - M_{app}|} \quad (2.12)$$

$$E_{12} = \frac{-(K_\theta V e m) - [V S \bar{q} [C_{L\alpha} (J + e^2 - m e e_{ac}) - C_{m\alpha} \bar{c} e m]]}{|M_s - M_{app}|} \quad (2.13)$$

$$E_{21} = \frac{-K_h (V m e + C_{L\dot{\alpha}} S \bar{q} e_{ac} + C_{M\dot{\alpha}} S q c)}{|M_s - M_{app}|} \quad (2.14)$$

$$E_{22} = \frac{-K_\theta (V m + C_{L\dot{\alpha}} S \bar{q}) - [S^2 \bar{q}^2 \bar{c} (C_{L\alpha} C_{m\alpha} - C_{L\dot{\alpha}} C_{M\dot{\alpha}}) s \bar{q} V m [C_{L\alpha} (e - e_{ac}) - C_{m\alpha} \bar{c}]]}{|M_s - M_{app}|} \quad (2.15)$$

$$|M_s - M_{app}| = J V m + \bar{q} S [C_{L\dot{\alpha}} (J + e^2 - m e e_{ac}) - C_{m\dot{\alpha}} \bar{c} e m] \quad (2.16)$$

Rotational stiffness only affects the elements E12 and E22, and can be separated out into the elements

$$E_{12L} = \frac{-[V S \bar{q} [C_{L\alpha} (J + e^2 - m e e_{ac}) - C_{m\alpha} \bar{c} e m]]}{|M_s - M_{app}|} \quad (2.17)$$

$$E_{22L} = \frac{-[S^2 \bar{q}^2 \bar{c} (C_{L\alpha} C_{m\alpha} - C_{L\dot{\alpha}} C_{M\dot{\alpha}}) s \bar{q} V m [C_{L\alpha} (e - e_{ac}) - C_{m\alpha} \bar{c}]]}{|M_s - M_{app}|} \quad (2.18)$$

and

$$E_{12N} = \frac{-(K_\theta V e m)}{|M_s - M_{app}|} \quad (2.19)$$

$$E_{22N} = \frac{-K_\theta(Vm + C_L \dot{\alpha} S \bar{q})}{|M_s - M_{app}|} \quad (2.20)$$

The state space representation in equation 2.11 becomes:

$$\dot{x}_1 = x_3 \quad (2.21)$$

$$\dot{x}_2 = x_4 \quad (2.22)$$

$$\dot{x}_3 = E_{11}x_1 + (E_{12L}x_2 + E_{12NL}\widehat{x}_2) + D_{11}x_3 + D_{12}x_4 \quad (2.23)$$

$$\dot{x}_4 = E_{21}x_1 + (E_{22L}x_2 + E_{22NL}\widehat{x}_2) + D_{21}x_3 + D_{22}x_4 \quad (2.24)$$

The equations above can express in matrix form

$$\dot{x}_1 = \begin{bmatrix} 0 & I \\ E_L & D \end{bmatrix} x + E_{NL}\widehat{x}_2 \quad (2.25)$$

The term above 2.25 can be simplified to nominal state equation, and  $\widehat{x}_2$  is now defined as  $\emptyset(\theta)$  and the state variable is defined as  $\theta = x_2 = [0 \ 0 \ 1 \ 0]x^T$ . The baseline state space formulation for nonlinear system is produced as follow:

$$\dot{x} = Ax + B\emptyset(\theta) \quad (2.26)$$

$$\theta = y = Cx \quad (2.27)$$

In this form, the stiffness constant in pitch,  $K_\theta$  is replaced with a general nonlinear function  $\emptyset(\theta)$  (Asjes, 2015).

## **CHAPTER 3**

### **METHODOLOGY**

This chapter presents the methodology employed in this work. The experimental work involved design, fabrication and wind tunnel testing of a 2 degree of freedom flutter system. Once flutter has been achieved, an active flutter suppression system was installed for evaluation. The objective of the evaluation is to test whether the suppression system using aileron control via a microcontroller (Autopilot) is able to suppress the flutter oscillations. The overall work flow described is shown in Figure 3.1. The wind tunnel aeroelastic flutter setup consists of a wing section and the elastic setup.